J. Electrochem. Sci. Eng. **00(0)** (2022) 000-000; http://dx.doi.org/10.5599/jese.1260

Open Access : : ISSN 1847-9286

www.jESE-online.org

Original scientific paper

Fabrication of superhydrophobic surfaces by laser surface texturing and autoxidation

Vijay Kumar✉, Rajeev Verma and Harish Kumar Bairwa

Industrial and Production Engineering Department, Dr B R Ambedkar National Institute of Technology Jalandhar, Punjab, India-144011

Corresponding author: ✉vknitj94@gmail.com

Received: January 7, 2022; Accepted: March 11, 2022; Published: May 4, 2022

Abstract

*The creation of superhydrophobic surfaces (SHS) has received exceptional thought from the entire research community due to its notable application in varied fields such as anti-icing, self-cleaning, drag reduction, anti-bacterial, and oil-water separation. The superhydrophobic (SH) conditions for a surface can be attained through the consolidation of a low surface energy surface with appropriate micro/nano-surface roughness through texturing. Motivated by the SH nature of lotus leaf and petal effect, microstructures have been prepared in this work on a metal surface by a fiber laser marking machine at 35 W. The textured surfaces with a different pitch to diameter (*p/d*) ratio (2.0-0.70) have been turned into hydrophobic and finally SH, after storing in an ambient environment for a few days due to oxide layer deposition on the textured surface. In this study, the maximum contact angle achieved by textured geometry after 30 days of auto-oxidation was 158.6 °. Further, test results showed that the fabricated surfaces have a high potential to maintain their SH nature even after the harsh condition of applications.*

Keywords

Anti-bacterial; oxide layer deposition; texturing; micro/nano-structure; self-cleaning

Introduction

Recently, the transformation in the wettability condition of metallic surfaces from hydrophilic to superhydrophobic (SH) has received considerable attention from researchers due to its numerous applications such as an anti-bacterial layer, anti-frosting, self-cleaning, and drag-reducing overlay [1]. The micro/nanostructures of insect wings and plants leaf have been saved as biomedical bodies for researchers to create such surfaces on metallic/alloy surfaces primarily to reduce maintenance costs. They show unique wetting behaviours such as SH and oil-water separation properties. The wettability behaviour of SHS is likely to be influenced by the micro/nano dual structure as well as the surface chemistry of the substrate surface [2].

The surface wettability can be categorized into three categories: hydrophilic, hydrophobic, and SH properties, which depend on the water contact angle (WCA) of the surface [3]. That is, the surface with WCA less than 90º is a hydrophilic surface, WCA lies between 90 to 150º for a hydrophobic surface, whereas WCA greater than 150º is referred to as SHS. The above states of the surface are highly influenced by the surface interface energy of water droplets and solid surfaces. The wettability of surfaces has been studied by three states: the Wenzel state, the Cassie-Baxter (CB) state, and the metastable state [4,5]. The Wenzel model considers water droplets seeping between surface asperities, while the CB model discusses water droplets settling onto irregularities and trapped air in the rough surface irregularities [6]. The schematic diagram of the above three categories is shown in Figure 1. Among the above three infiltration states, the CB state is more appropriate for the investigation of the SHS [7,8] since it is valid for rough and chemically homogeneous surfaces and to air entrapment inside the irregularities of rough surfaces.

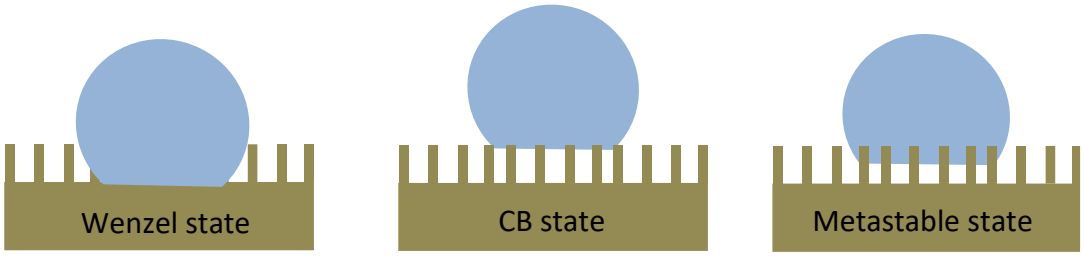

Figure 1. *Infiltration states in Wenzel, CB and metastable states*

SHS has the potential application to reduce corrosion behavior and is advantageous in self-cleaning and offers antiseptic environments [9]. There are two essential aspects to enhancing the SH behaviour of a surface that is low surface energy treatment and the creation of micro/nano-hierarchical structure. To improve the intrinsic SH behaviour of the surface, laser surface texturing has been a relatively new technique for creating a dual structure on metallic surfaces, which is responsible for the making surface non-sticky. So far, to produce such micro/nano-dual scale structures on a surface, a great effort has been made lately by researchers and this has been a motivation to discover a newer technique, which is easy and eco-friendly [10]. Previously, several techniques have been proposed and investigated to achieve high WCA and low CA hysteresis, such as chemical etching [11], plasma etching [12], shot blasting [13], machining [14], lithographic patterning [15], sol-gel technique [16], electrodeposition [17], and plasma fluorination technique [18]. However, the previously reported techniques have some disadvantages that limit their application, for example, the intricate processing steps and low durability. To create SHS, some chemical modifications such as coating of fluorosilane and fluoropolymer are used as the top layer, which significantly improves the hydrophobic behavior of the surface [19]. However, these fluorinated coatings are harmful to the environment and also may be easily peeled off from the substrate interface due to poor mechanical interlocking and thermal stability. To overcome the above shortcomings, laser surface texturing has emerged as one of the best techniques to produce a hierarchical structure with well-defined surface roughness as a requisite favorable condition for attaining SH behavior. Laser texturing produces required surface roughness and spontaneous hydrophobization and carbon absorption onto the textured surfaces with a multimodal roughness that looks passive, environmentally friendly, and naturally reproducible [20]. Recently, Ma *et al*. fabricated SHS by creating a circular texturing pattern of different *p*/*d* ratios, which were highly durable [21]. Moreover, creating an SHS by optimizing *p*/*d* ratios for different materials became an interesting area for researchers due to its high durability and eco-friendly nature.

Very little literature has been reported on the fabrication of SHS by direct laser treatment on steel surfaces. The fabrication of superhydrophobic or hydrophobic surfaces by direct laser texturing (DLT) eliminates the use of any hazardous chemical treatment. The creation of SHS by DLT and deposition of oxide layer due to heat-treatment during texturing (autoxidation) is highly responsible for better durability and maintaining their behavior against harsh environmental conditions.

In this work, the fiber laser marking machine of 50W was employed to create a micro/nano-hierarchical structure on AISI 420 steel substrate. To attain a stable SH condition, the textured surfaces of different *p*/*d* ratios such as 2.0, 1.0, 0.95, 0.90, 0.80, and 0.70 were left in an open environment for a few days. The surface characterization through scanning electron microscopy analysis, tape peel test, and sandpaper abrasion test were employed to evaluate the soundness of the developed SHS.

Experimental

Surface preparation

The AISI 420 steel plate was procured from the local market of Jalandhar and its chemical composition was evaluated by spectroscopic analysis at the Central Institute of Hand Tools, Jalandhar, Punjab, India (Table 1). To perform micro-texturing on the AISI 420 steel sheet was sectioned to the size of 40×40×5 mm. Subsequently, the sectioned surface was polished with abrasive sandpaper of P200, P400, P800, P1200, and P1500 followed by washing with ethanol and deionized water. Before laser texturing, all samples were dried in an electric oven at 80 °C for 30 minutes to remove moisture from the surfaces.

***Table 1**. Spectroscopic analysis of AISI 420 steel*

Element	C	Cr	Mn	Si	P	S	Fe
Content, wt.%	0.13	12.60	0.85	0.73	0.03	0.05	Balance

Laser surface texturing

The fiber laser marking machine (Figure 2) with a 50 W laser source was applied to micro-texture the circular pattern of diameter 100 µm and pitch varying from 200 to 70 µm as tabulated in Table 2.

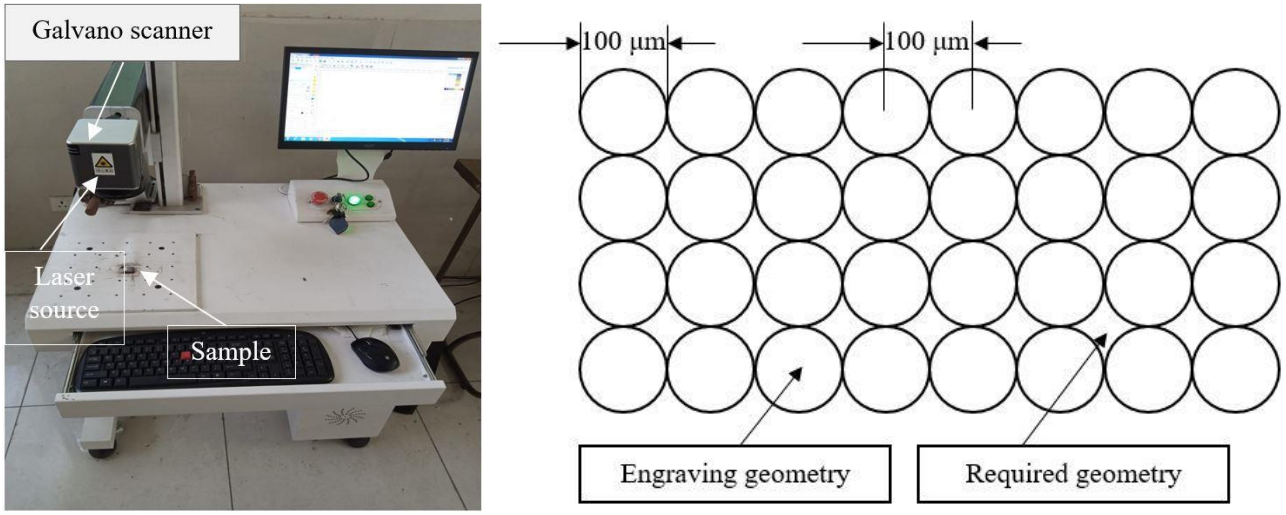

***Figure 2.** Laser texturing machine and its texturing parameters (EzCad software)*

The scanning speed used was 50 mm/s, a frequency of 50 kHz, and a maximum power of 35 W with a laser wavelength of 1064 nm. The same parameters were repeated three times for every sample to achieve the surface roughness (R_a) between 8 and 14 μm, as seen in Table 2. From Table 2, it has been observed that Ra values of the textured geometry increase with a decrease in *p*/*d* ratio, which could be ascribed to the decrease in the flat area of the textured geometry. With the increase of the *p*/*d* ratio, the untextured surface area (outside the cylinder) increases, and the mean surface roughness decreases.

Table 2*. Parameters of texturing pattern and its surface roughness values, d = 100 μm*

Sample No.	*p* / μm	*p* /*d*	R_a / μm
1	200	2	9.10
2	100	1.00	9.15
3	95	0.95	9.79
4	90	0.90	10.23
5	80	0.80	11.02
6	70	0.70	11.29

Surface characterization

The surface morphology of the textured surface was characterized using scanning electron microscopy (SEM). The wettability and durability of the texture geometry were investigated by assessing the mechanical resistance by a small-scale laboratory testing, such as tape peeling, abrasive paper abrasion, and contact angle hysteresis of water droplets deposited on the textured surface. The droplet contact angle is defined as the angle at which the water-air interface intersects the surface, which characterizes the wettability tendency of liquid droplets. The roll-off angle represents the slope of a surface from that a drop starts rolling and eventually falls. Wettability conditions of superhydrophobicity are usually accepted when the contact angle is greater than 150^o and also the roll angle is lower than 10^o [22]. The WCA value has been measured for each experiment and co-related with the SEM topography and the degree of hydrophobicity. We used a technique like a sessile contact angle approach and for this purpose, an image was captured of liquid droplets on the textured surface using a high-resolution (micro-lens) camera. Then the image processing was carried out to assess the contact perspective as described above. Depending on the degree of rolling, we incrementally tilted the samples to determine the angle when the drop started rolling off from the surface. For this purpose, a drop of water of 10 μl volume was released from a micro-syringe from a height of 10 mm, and the drop image was captured and analyzed using image analysis software under ambient conditions (at 5-days interval).

Mechanical testing

Tape peel test

Generally, a tape peeling test is carried out to investigate the behavior of superhydrophobic surfaces after being glued to other surfaces, which indicates the loss of a degree of wettability of the SH surface. For the tape-peeling test, the highly adhesive and pressure-sensitive tape is used for uniformity of adhesion. In this work, Cellofix test tapes were used for uniformly adhering to the textured surface with the application of an external load of 80 g rolling onto the entire surface for proper adherence with the SH surface. The glued tape was later lifted at an angle of 180^o to the surface [8,10,23]. The wettability of the surfaces was measured after every 10 repetitions of the test. This test was measured until the SH surface showed very low wettability loss.

Sandpaper abrasion test

A sandpaper abrasion test was carried out to evaluate the durability of the SH surfaces against the damage from abrasive particles, which shows the wettability changes after a number of abrasion cycles. In this test, the sandpaper of grit size P800 was put on the SH surface to a length of 40 mm facing abrasive particles towards the SH surface. Applied 100 g external load on top of the sandpaper and sandpaper was pulled horizontally with a constant velocity of approximately 10 mm/s. This test was repeated for 50 cycles and the WCA of abraded surfaces was measured at intervals of 10 abrasion cycles [24-26].

Results and discussion

In the present experiment, we have successfully produced metal textured surfaces with uniform SH properties using laser texturing (Figure 3).

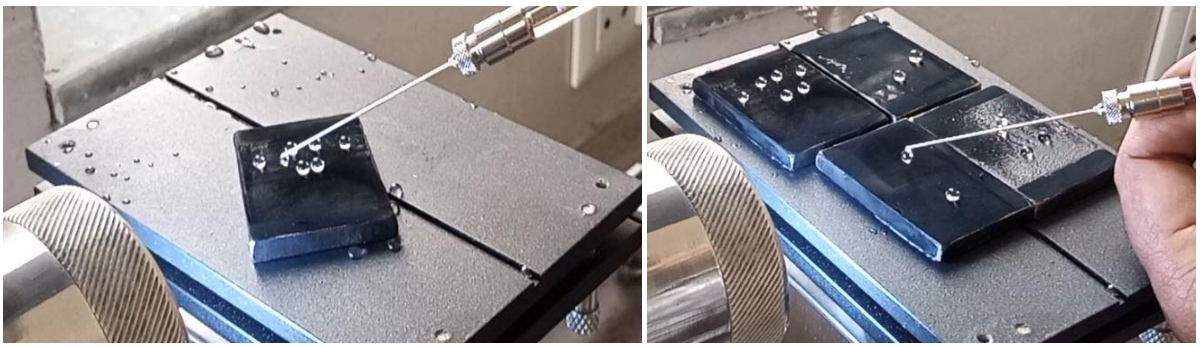

Figure 3*. Water droplets exhibiting uniform hydrophobic and SH properties of textured surfaces after 19 days of exposure to the open environment*

Influence of laser texturing on surface morphology

It has been well established that the morphology of the surface and the roughness have a strong influence on surface wettability. In general, it has been reported in the literature that two states, namely Wenzel and Cassie-Baxter (CB), are used to explain the liquid-solid interaction: (1) the liquid fills the valleys of a rough solid surface known as the Wenzel state, and (2) air entering the valleys of the rough solid surface called CB state. When processing line by line (two laser beams separated by distance) during laser texturing, the laser beams move and remove material (ablation) from the surface by melting and evaporating the metal, creating micro-patterned structures. To produce metallic surfaces with SH properties, the surface must become one of three structures: nanostructures, microstructures, or dual structures [27]. In this work, the circular-shaped texturing with different *p*/*d* ratios (2.0-0.7) was fabricated on steel samples by a fibre laser texturing machine. During pilot experimentation, SH behaviour on the samples was performed to optimize the *p*/*d* ratio. From the study, it was found that textured geometry with a *p*/*d* ratio of 0.7 resulted in the maximum WCA, demonstrating the most encouraging results, whereas textured geometry with a *p*/*d* ratio 2 and more did not show many promising WCA results due to more flat surfaces present on top of the sample. Based on this preliminary study, our further investigation was mainly focused on textured geometry with a *p*/*d* ratio of 0.7, and a sample of texturing with a *p*/*d* ratio of 2 was discarded from the further investigation.

A distribution of multi-model and regular pattern geometry has been produced after laser texturing, as shown in the SEM image of the textured substrates at different magnification levels. The laser-processed substrate surface produced a hierarchical structure, a nanostructure in micro-protrusion pores and depressions, due to the evaporation and inherent laser bulging effect.

Figure 4 shows the SEM image of the texture pattern structure with a *p*/*d* ratio of 0.7 at magnification levels of 200× and 500×, respectively. The SEM images show the formulation of a coral-like surface structured with mushroom-like nano-protrusions on micro-cavities arranged in random alignments. These uniform/deterministic micro-cavities-oriented structures consisted of tiny cavities with dimensions in the micron to nano range that created an ultrafine porous structure [28]. Further studies show that these structures were reproducible and well controllable by adjusting the laser parameters. After the laser ablation process, the WCA on all textured geometries was measured and left at ambient conditions to further study the wettability behaviour with time. Further investigation of WCA ensured that the surface wettability of laser-ablated surfaces increases with time.

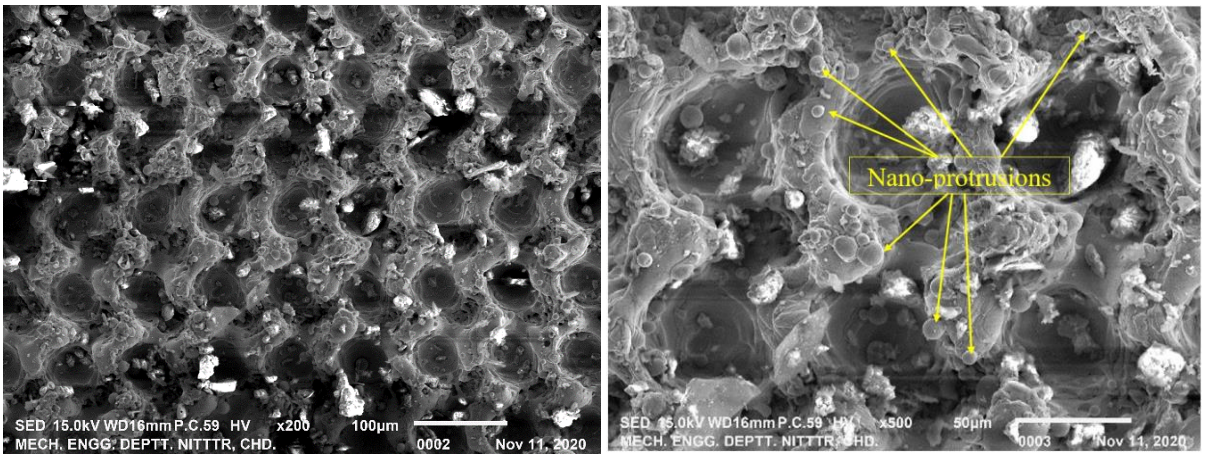

Figure 4. *SEM images of a textured surface with a* p/d *ratio of 0.7 at different magnification levels*

Effect of auto-oxidation on wettability

The topography of the textured surface depends on the laser power and the intensity of the beam. It is well known that spatial depth and heat zone increase with increasing laser intensity. As the laser intensity doubles, the heat-affected region lengthens three times. The result is that the texturing pattern's size increased and a distorted type of heat-affected zone was created [2,29]. One advantage of pattern distortion is that it creates a nano protrusion and a high heat-affected zone is highly responsible for the oxide formation and carbon abstractions from the environment and surface dissolution. After laser texturing on the specimens, WCA was measured on the textured patterns and all specimens were subjected to exposure to an open environment for further wettability studies time the contact angle was measured at time intervals of five days, as shown in Table 3.

Table 3*. Wettability measurement on the laser texture AISI 420 steel*

	p / *d*				
	0.7	0.8	0.9	0.95	1.0
Time interval. day	WCA, °				
1	97.90	85.36	77.23	70.9	70.2
5	125..42	101.21	92.32	88.12	86.3
10	131.48	115.23	105.41	100.32	98.25
15	145.49	129.3	121.23	114	101
19	158.59	135.23	123	114.45	101

After 15 days, it was observed as 145.45° and after 19 days, the fabricated surface showed SH behaviour with a contact angle of 158.6° in textured geometry with a *p*/*d* ratio of 0.7, whereas no significant change in the contact angle was observed after 19 days, as shown in Figure 6. The

variation in wettability over time is due to a change in surface chemistry and a key factor could be ascribed to the accumulation of carbon to the textured substrate with active magnetite, as shown in Table 4 [30]. This accumulation of carbon particles from the air on the textured geometry and air entrapment inside the texturing pattern creates low surface energy on the surfaces. As a result, when a higher energy liquid is dropped on this surface, it is repelled from the surface and tries to attain a spherical shape due to the dominant molecular cohesive forces among the water droplets. Further, it was observed, that after a small surface inclination, the water droplets roll off easily from the surfaces. The EDS analysis of textured geometry with a *p*/*d* ratio of 0.7 (Figure 5) after 19 days shows an enormous chemical composition alteration of the surface, as shown in Table 4. The higher chemical composition alteration especially carbon and oxygen, may be caused due to surface burring due to ablation during laser texturing and oxidation due to heat treatment during texturing followed by auto-oxidation. From Table 4, trends of increasing percentage composition of lower melting points elements have been observed after laser texturing. This may be due to the lower melting points element diffusing out to the surface by heat treatment during texturing due to high laser fluence. The high increment of carbon composition and introduction of oxide formation on the textured geometry could be accounted for by the creation of low surface energy.

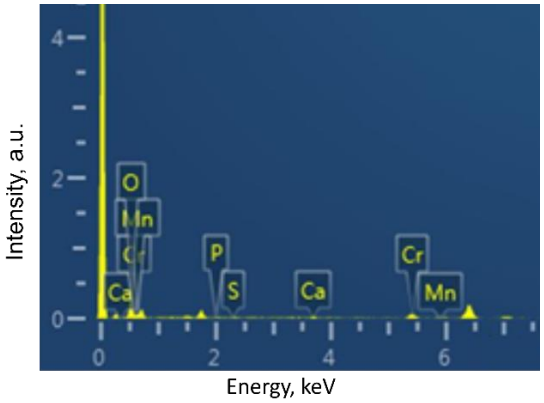

***Figure 5**. Energy-dispersive X-ray spectroscopy (EDS) on the textured surface*

***Table 4.** Chemical composition of texture surface before and after texturing*

Before texturing		After texturing	
Element	Content, wt. %	Element	Content, wt. %
C	0.13	C	6.35
P	0.035	P	0.33
S	0.026	S	0.44
Si	0.59	Si	4.58
Cr	13.68	Cr	9.67
Fe	84.56	Fe	59.61
		O	17.47
		Ca	1.55
Total	100.00		100.00

Micrographs of the SHS were examined by SEM and EDS analysis at 10 kV at the NITTR in Chandigarh, India, to examine the surface morphology and chemical composition of the surfaces. The ability of water repellence increases with decreasing *p*/*d* value of the laser-ablated surface due to increased surface roughness and the same behaviour for the other values of the *p*/*d* ratio was observed. There was no significant change in the contact angles of the irradiated surface with time after a stable equilibrium was reached. The WCA of water droplets was calculated on laser irradiated surfaces (*p*/*d* = 0.7, 0.8, 0.90, 0.95, and 1.0) ablated with the same laser fluence and left at ambient conditions for 19 days. It could be acknowledged from the results obtained that the pulse superposition implemented in the ablation process could play an essential role in the surface topography produced by the laser texturing process. As the *p*/*d* ratio of the circular texture pattern decreased from 1.0 to 0.7, the surface roughness (9.15 µm to 11.29 µm) also increased as shown in Table 2. The increase of Ra value with dual structure is highly responsible for the improvement in hydrophilic to SH behaviour. Further, with the increase of the *p*/*d* ratio from 0.7 to 2.0, the surface microstructure becomes very flat and there are not many nano-scale multi-modal structures present on the surface to offer hydrophobicity. The decrease in CAs and the high adhesive force of these surfaces can be explained according to the Wenzel model. As illustrated in Figure 6, the lower WCA

on textured geometry except/compared to *p*/*d* ratio 0.7 was due to the water droplet could get into the groove of the rough solid surface partially or completely.

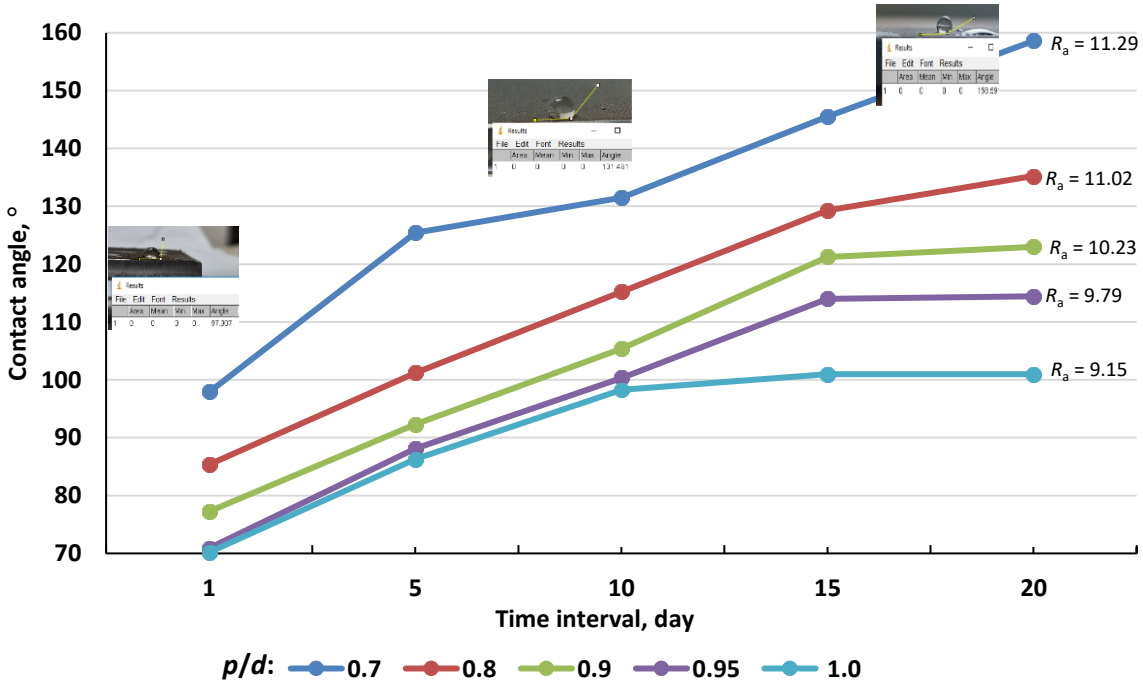

***Figure 6**. WCA of textured AISI 420 steel specimens with different* p/d *ratios during 20 days interval*

Mechanical test

To determine the functional working efficiency of the fabricated SHS, mechanical reliability is also a critical parameter. In general, the SHS artificially produced by chemical methods are relative of low durability and can lose their ability to repel water through scratching or abrasion, causing excessive damage to the surface chemistry and structure [24]. Small scale laboratory tests prevalent to ascertain the durability of SHS were conducted, namely sandpaper abrasion tests, tape peel tests, and water repellency over time. In this study, SH surfaces show marginal loss of wettability after 50 test repetitions. It was observed that samples with a *p*/*d* ratio of 0.7 had exhibited some decreasing trend of WCA during the first 40 test cycles of the tape peel test and a similar diminishing trend was observed in the sandpaper abrasion test. A very small wettability change of the surface had been observed in the first 10 cycles of the abrasive paper scratch test. Whiles, a sharp drop in WCA (Figure 7) from 157.40 to 144.30 was observed between 10 to 50 cycles as the structure of the textured substrate was damaged. The decreasing trends of WCA were observed after increasing the number of testing cycles because when the number of cycles increases, the nano-protrusion over micro-structures gets damaged after every repetition. However, the surface remains hydrophobic after 50 cycles of test and it marginally lost its ability to repel water.

The promising results of the study show that these low water adhesion SHS can be used in many engineering fields, such as the 'mechanical hand' to transfer small water droplets without any loss or contamination for micro sample analysis. These SHS can also be used to store any type of liquid solution in small volumes where no loss is required. Moreover, such surfaces can also be used to transfer liquid droplets from low adhesion surface to high adhesion surface without any loss.

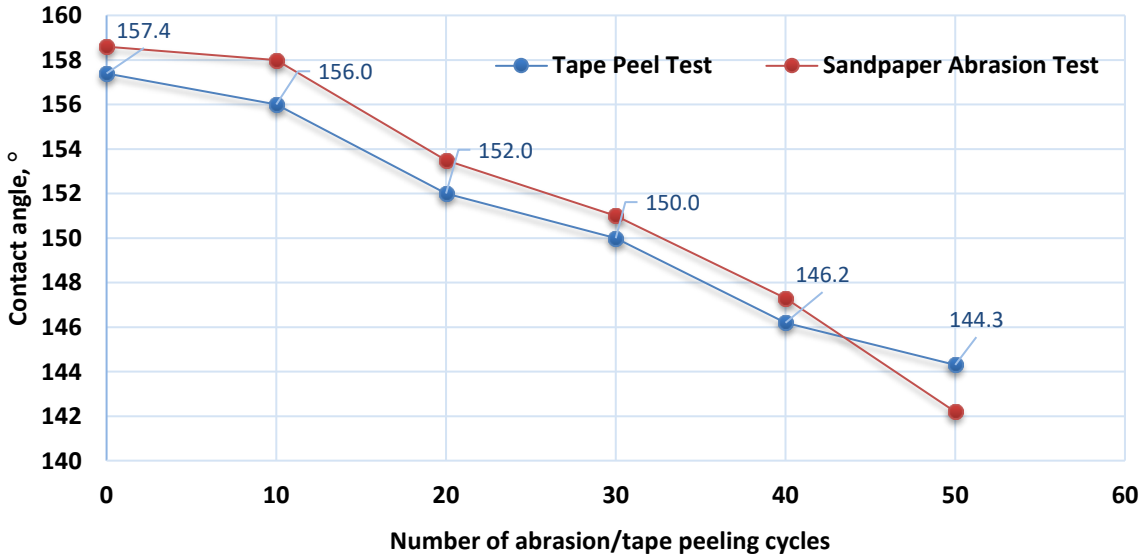

***Figure 7**. WCA measurement on the surface after mechanical testing (p/d = 0.70)*

Conclusion

It has been shown that a compact and relatively inexpensive fiber laser texturing machine can be used to produce SHS on AISI 420 steel substrates that exhibit hydrophobic properties immediately after direct laser texturing under atmospheric conditions. The wettability of the ablated surface enhances with time and the surfaces become SH after 19 days of autoxidation. To evaluate the mechanical stability of the developed SHS, two different test methods were performed, the first being the sandpaper abrasion test and the second being the tape-peel adhesion test. Following are the main finding of the study:

- SEM and EDS analysis showed that laser texturing was mainly responsible for the changes in surface morphology and scatting surface chemistry. The results showed that both the surface chemistry and the pulse overlap could have a significant impact on the water repellency of the AISI 420 steel surface.
- The superhydrophobicity of the laser-textured surface increased with decreasing *p*/*d* value due to increased surface roughness. A circular texture pattern with a value of 0.7 *p*/*d* shows excellent non-wetting behaviour due to increased surface roughness. The maximum WCA achieved was 158.6^{o} after 19 days of the sample stored at ambient conditions.
- After investigation, it has been found that an increase in carbon and oxidation percentage on the textured surface over time was highly responsible for the SH behaviour.

References

[1] B. D. Rezgui, *Surface Texturing for a Superhydrophobic Surface,* in: *The Effects of Dust and Heat on Photovoltaic Modules: Impacts and Solutions,* A. Al-Ahmed, Inamuddin, F.A. Al-Sulaiman, F. Khan (Eds.), Green Energy and Technology, Springer Cham, 2022, p. 113. https://doi.org/10.1007/978-3-030-84635-0_5

[2] Z. Yang, C. Zhu, N. Zheng, D. Le, J. Zhou, *Materials (Basel)* **11(11)** (2018) 2210. https://doi.org/10.3390/ma11112210

[3] Y. Wang, J. Liu, M. Li, Q. Wang, Q. Chen, *Applied Surface Science* **385** (2016) 472-480. https://doi.org/10.1016/j.apsusc.2016.05.117

[4] H. H. Nguyen, A. K. Tieu, S. Wan, H. Zhu, S. T. Pham, B. Johnston, *Applied Surface Science* **537** (2021) 147808. https://doi.org/10.1016/j.apsusc.2020.147808

[5] A. R. Esmaeili, N. Mir, R. Mohammadi, A Facile, *Journal of Colloid and Interface Science* **573** (2021) 317-327. https://doi.org/10.1016/j.jcis.2020.04.027
[6] Y. Cho, C.H. Park, *RSC Advances* **10(52)** (2020) 31251-31260. https://doi.org/10.1039/D0RA03137B
[7] V. Kumar, R. Verma, S. Kango, V.S. Sharma, *Materials Today Communications* **26** (2021) 101736. https://doi.org/10.1016/j.mtcomm.2020.101736
[8] V. Kumar, R. Verma, S. Kango, *Transactions of the Indian Institute of Metals* **73** (2020) 1025-1026. https://doi.org/10.1007/s12666-020-01918-8
[9] B. S. Yilbas, H. Ali, A. Al-Sharafi, N. Al-Aqeeli, *Optics and Lasers in Engineering* **102** (2018) 1-9. https://doi.org/10.1016/j.optlaseng.2017.10.014
[10] R. S. Sutar, S. S. Latthe, S. Nagappan, C.-S. Ha, K. K. Sadasivuni, S. Liu, R. Xing, A. K. Bhosale, *Journal of Applied Polymer Science* **138(9)** (2021) 49943. https://doi.org/10.1002/app.49943
[11] J. Wu, J. Chen, J. Xia, W. Lei, B.-p. Wang, *Advances in Materials Science and Engineering* **2013** (2013) 232681. https://doi.org/10.1155/2013/232681
[12] K. Ellinas, A. Tserepi, E. Gogolides, *Langmuir* **27(7)** (2011) 3960-3969. https://doi.org/10.1021/la104481p
[13] G. Deep, V. Rajora, I. Singh, *3rd National Conference on Advancements in Simulation & Experimental Techniques in Mechanical Engineering (NCASEme-2016)*, *Proceedings*, Chandigarh University, Gharuan, Mohali, Punjab, India, 2016, p. 253-257.
[14] D-M. Chun, C.-V. Ngo, K.-M. Lee, *CIRP Annals - Manufacturing Technology* **65(1)** (2016) 519-522. https://doi.org/10.1016/j.cirp.2016.04.019
[15] K. Ellinas, M. Chatzipetrou, I. Zergioti, A. Tserepi, E. Gogolides, *Advanced Materials* **27(13)** (2015) 2231-2235. https://doi.org/10.1002/adma.201405855
[16] X. Wu, V. V. Silberschmidt, Z.-T. Hu, Z. Chen, *Surface and Coatings Technology* **358** (2019) 207-214. https://doi.org/10.1016/j.surfcoat.2018.11.039
[17] H. M. Forooshani, M. Aliofkhazraei, H. Bagheri, *Journal of Alloys and Compounds* **784** (2019) 556-573. https://doi.org/10.1016/j.jallcom.2019.01.079
[18] D. Zhao, M. Pan, J. Yuan, H. Liu, S. Song, L. Zhu, *Progress in Organic Coatings* **138** (2020) 105368. https://doi.org/10.1016/j.porgcoat.2019.105368
[19] Y. Xiu, L. Zhu, D.W. Hess, C. P. Wong, *Nano Letters* **7(11)** (2007) 3388-3393. https://doi.org/10.1021/nl0717457
[20] L. B. Boinovich, A. M. Emelyanenko, K. A. Emelyanenko, A. G. Domantovsky, A. A. Shiryaev, *Applied Surface Science* **379** (2016) 111-113. https://doi.org/10.1016/j.apsusc.2016.04.056
[21] Q. Ma, Z. Tong, W. Wang, G. Dong, *Applied Surface Science* **455** (2018) 748-757. https://doi.org/10.1016/j.apsusc.2018.06.033
[22] S. Niu, B. Li, Z. Mu, M. Yang, J. Zhang, Z. Han, L. Ren, *Journal of Bionic Engineering* **12(2)** (2015) 170-189. https://doi.org/10.1016/S1672-6529(14)60111-6
[23] T. Wu, W.-hua Xu, K. Guo, H. Xie, J.-ping Qu, *Chemical Engineering Journal* **407** (2021) 127100. https://doi.org/10.1016/j.cej.2020.127100
[24] X. Gao, Z. Guo, *Journal of Colloid and Interface Science* **512** (2018) 239-248. https://doi.org/10.1016/j.jcis.2017.10.061
[25] Y. Zhang, L. Zhang, Z. Xiao, S. Wang, X. Yu, *Chemical Engineering Journal* **369** (2019) 1-7. https://doi.org/10.1016/j.cej.2019.03.021
[26] R. S. Sutar, S. S. Latthe, A. M. Sargar, C. E. Patil, V. S. Jadhav, A. N. Patil, K. K. Kokate, A. K. Bhosale, K. K. Sadasivuni, S. V. Mohite, S. Liu, R. Xing, *Macromolecular Symposia* **393(1)** (2020) 2000031. https://doi.org/10.1002/masy.202000031
[27] Y. Yoon, D. Kim, J.-B. Lee, *Micro and Nano Systems Letters* **2(1)** (2014) 3. https://doi.org/10.1186/s40486-014-0003-x

[28] E. Liu, H.J. Lee, X. Lu, *Applied Sciences (Switzerland)* **10(8)** (2020) 2678. https://doi.org/10.3390/app10082678
[29] V. Kumar, R. Verma, V.S. Sharma, V. Sharma, *Surface Topography: Metrology and Properties*, **9(4)** (2022) 43003. https://doi.org/10.1088/2051-672X/ac4321
[30] Y. Liu, H. Gao, S. Li, Z. Han, L. Ren, *Chemical Engineering Journal* **337** (2018) 697-708. https://doi.org/10.1016/j.cej.2017.12.139